A Robust Beamforming Algorithm for Satellite Communication

Ruonan Yang[1], Ying Chen[1(✉)], Chuili Kong[1], Rong Li[1], Jun Wang[1], and Kai Wang[2]

[1] Huawei Technologies Co., Ltd., Hangzhou, China
chenying18@huawei.com
[2] PengCheng Laboratory, Shenzhen, China
wangk01@pcl.ac.cn

Abstract. The triangular lattice is preferred in the case when the available estate is limited, since it entails a higher element density than that obtainable with a square lattice of identical inter-element distance. However, the antenna pattern of the triangular lattice is very sensitive to the change of the beam pointing direction due to its nonuniform distribution of beam gain, which probably results in a large SNR decrease with a minor beam pointing error. To address this issue, in this paper, we focus on the two dimensions, i.e., the elevation angle and the azimuth angle, and propose an adaptive azimuth adjustment algorithm to overcome the performance loss caused by the unpredictable elevation angle's variation. Simulation results reveal that the total SNR reduction is less than 0.18dB when the elevation angle changes up to $\pm 5^{\circ}$, which demonstrates the robustness of our proposed algorithm.

Keywords: Beamforming · Triangular lattice antenna · Satellite communication

1 Introduction

With the breakthrough of satellite manufacturing and launching technologies in recent years, the Low Earth Orbit (LEO) satellite system is widely investigated as a part of the 6G network [1–3]. It not only provides communications with broadband and wide range IoT services around the world, but also brings other new functions such as precision enhanced positioning, navigation, and real time earth observation, with the potential of seamless coverage of the earth in a cost effective way.

For LEO satellite, the link budget is normally limited due to the large propagation loss. Thus, it is natural to use antenna arrays at satellite to provide a directive beam to User Equipment (UE) and, at the same time, suppress the radiation in other directions. Alternatively, the directive beam can be generated by a phased antenna array. To enforce a desired far field pattern, each location and feeding of individual elements in the antenna array is properly selected. Typically, the operative multibeam satellite systems usually employ four color frequency reuse to reduce the interbeam interference (IBI) and multibeam pre-

J. Zhao (Ed.): WiSATS 2023, LNICST 509, pp. 94–105, 2023.
https://doi.org/10.1007/978-3-031-34851-8_8

coding for the same color. In terms of the beam associated way, moving beams and earth-fixed beams are discussed by the 3rd Generation Partnership Project (3GPP). In the moving beam system, the beam directions are unchanged, and hence the beam footprint on earth is moving fast at the same speed level of the satellite. Therefore, even though the position of a UE is fixed, its serving beam is always changing, which causes large signaling overhead by frequent handover and a large Signal-to-Noise Ratio (SNR) change. In contrast, the beam direction always points to the UE in the earth-fixed beam system [4,5], which ensures a reduced handover rate, and low SNR variation. Motivated by this, in this paper, we focus on the earth-fixed beam system.

In most of the planar array layout studied thus far in literature, there are two frequently used cases, namely, square and triangular lattice arrays. The former's antenna elements are deployed on a regular square grid, whereas the latter elements are on a regular triangular grid. Given the same inter-element distance, the triangular lattice entails a higher element density than the counterpart of the square lattice, which indicates a smaller array size [6–10]. Therefore, the triangular lattice is preferred in satellite systems since it at some extent reduces the size and weight of the satellite payload. However, the antenna pattern of the triangular lattice is very sensitive to the change of the beam pointing direction. Possible pointing error may be introduced due to random vibrations or movements of the telescope platform known as jitter, especially for limited size of satellite antenna aperture [11,12]. [13] presented a typical value of jitter in terrestrial system. For satellite communication system, it would be more serious. For example, with a small variation of the elevation angle, i.e., $\pm 5°$, the SNR decreases significantly, i.e., by approximately 2–6 dB. This loss is nontrivial especially for power-limited LEO satellite systems. Motivated by this, in this paper, we present a detailed performance investigation of the satellite system by considering the impact of the jitter. In particular, the main contributions are highlighted as follows:

- We first formulate the association between the Earth Centered Inertial (ECI) coordinate system and the local satellite's antenna system, which ensure that the satellite beams coverage a UE or a specific area on the earth, by taking the rotation of the earth into account.
- Then, we investigate the impact of the azimuth angle on the beam gain loss for a targeted UE when the satellite antenna's jitter occurs. Simulation results demonstrate that the jitter causes the SNR loss of 2–6 dB, which is highly undesirable for the very power-limited LEO satellite systems.
- Fortunately, we find an interesting phenomenon: for a certain target elevation, there is at least one best azimuth direction that can make the beam most tolerant for elevation variation. Based on this, we propose an adaptive azimuth adjustment algorithm to improve the robustness to the variation of elevation angle. Simulation results show that our proposed algorithm can at least guarantee the total SNR decreases no more than 0.18dB when the elevation angle change $\pm 5°$.

The rest of this paper is organized as follows. The system model and problem formulation are presented in Sect. 2. The robust beamforming algorithm is designed in Sect. 3. Simulation results are provided in Sect. 4. The conclusion is remarked in Sect. 5.

Notation: scalars are denoted by lower case italic letters $(a, b, ...)$, vectors by lower case boldface letters $(\mathbf{a}, \mathbf{b}, ...)$, and matrices by boldface capitals $(\mathbf{A}, \mathbf{B}, ...)$. Italic capitals are used to denote index upper bound $(k = 1, ..., K)$. The notation $\|\cdot\|$ denotes the Euclid norm. The cross product of $\mathbf{a}$ and $\mathbf{b}$ is indicated by $\mathbf{a} \times \mathbf{b}$, whereas the dot product is $\mathbf{a} \cdot \mathbf{b}$.

2 System Model

We consider a satellite communication network in the ECI coordinate system. As shown in Fig. 1, the Z-axis is pointed to the earth center, and the X-axis is the velocity vector, and Y-axis can be obtained by the right hand criterion. Therefore, the corresponding unit vectors of X-Y-Z axis can be written as

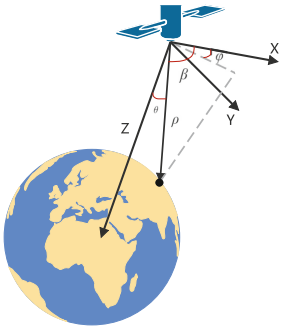

Fig. 1. Orbit coordinate system of the satellite.

$$\mathbf{r}_Z = -\frac{\mathbf{p}_s}{\|\mathbf{p}_s\|}; \mathbf{r}_X = \frac{\mathbf{v}_s}{\|\mathbf{v}_s\|}; \mathbf{r}_Y = \mathbf{r}_z \times \mathbf{r}_x \tag{1}$$

where $\mathbf{p}_s$ and $\mathbf{v}_s$ denote the position and velocity vector of the satellite. Thus the unit vector pointed from satellite to a UE located on the earth can be constructed as

$$\boldsymbol{\rho} = \frac{\mathbf{p}_s - \mathbf{p}_u}{\|\mathbf{p}_s - \mathbf{p}_u\|} \tag{2}$$

where $\mathbf{p}_u$ denotes the position of the UE. Let θ denote the elevation angle between the observed direction and XOY plane, and φ denote the azimuth angle between the projection on XOY plane of the observed direction and X axis. The corresponding elevation angle θ can be calculated as

$$\theta = \arccos \frac{\boldsymbol{\rho} \cdot \mathbf{r}_Z}{\|\boldsymbol{\rho}\| \|\mathbf{r}_Z\|} \tag{3}$$

Let β denote the angle between the vector ρ and X-axis, we have the following formula

$$\|\boldsymbol{\rho}\|\cos\beta = \|\boldsymbol{\rho}\|\sin\theta\cos\varphi \tag{4}$$

where $\cos\beta$ is calculated as

$$\cos\beta = \frac{\boldsymbol{\rho}\cdot\mathbf{r}_X}{\|\boldsymbol{\rho}\|\|\mathbf{r}_X\|} \tag{5}$$

Therefore, the value of φ can be obtained as

$$\varphi = \arccos\frac{\boldsymbol{\rho}\cdot\mathbf{r}_X}{\|\boldsymbol{\rho}\|\|\mathbf{r}_X\|\sin\theta} \tag{6}$$

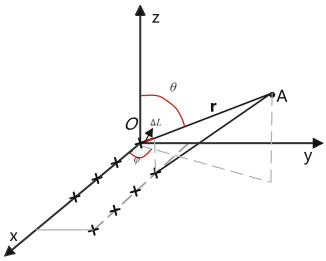

Fig. 2. Antenna coordinate system of a triangular grid array.

Suppose that a triangular grid array antenna with $N_x \times N_y$ elements as illustrated in Fig. 2. To describe the direction of the target UE clearly, let O-xyz denote the antenna coordinate system, the distance difference between the (i,j)-th element and the coordinate origin in space is

$$\triangle L = \frac{\mathbf{d}_{ij}\cdot\mathbf{r}}{\|\mathbf{r}\|} \tag{7}$$

where $\mathbf{d}_{ij}$ denotes the vector from the coordinate origin to the (i,j)-th element, and $\mathbf{r}$ is the unit vector from the coordinate origin to the target. If the antenna array is going to form a beam at (θ_0,φ_0), $\triangle L$ can also be written as

$$\triangle L = \|\mathbf{d}_{ij}\|_x\sin\theta_0\cos\varphi_0 + \|\mathbf{d}_{ij}\|_y\sin\theta_0\sin\varphi_0 \tag{8}$$

where $\|\mathbf{d}_{ij}\|_x$ denotes the length of the projection of $\mathbf{d}_{ij}$ on x axis and $\|\mathbf{d}_{ij}\|_y$ denotes the length of the projection of $\mathbf{d}_{ij}$ on y axis.

Consequently, the phase difference between the (i,j)-th element and the reference element at coordinate origin can be obtained by

$$\phi_{ij} = \frac{2\pi}{\lambda}\cdot(\|\mathbf{d}_{ij}\|_x\sin\theta_0\cos\varphi_0 + \|\mathbf{d}_{ij}\|_y\sin\theta_0\sin\varphi_0) \tag{9}$$

where λ is the wavelength. Then the pattern of the triangular lattice array antenna with $N_x \times N_y$ elements is given by

$$F_{\theta_0,\varphi_0}(\theta,\varphi) = \sum_{i=1}^{N_x}\sum_{j=1}^{N_y}\frac{1}{N_x \times N_y} W \cdot \exp(j\phi_{ij}) \tag{10}$$

where W is the phase excitation for different elements on the direction of θ, φ,

$$W = \exp\left[-j\frac{2\pi}{\lambda}\cdot(\|\mathbf{d}_{ij}\|_x \sin\theta\cos\varphi + \|\mathbf{d}_{ij}\|_y \sin\theta\sin\varphi)\right] \tag{11}$$

To simplify the expression of antenna pattern, $F_{\theta_0,\varphi_0}(\theta,\varphi)$ can be rewritten as

$$F_{\theta_0,\varphi_0}(\theta,\varphi) = \frac{1}{N_x \times N_y}\sum_{i=1}^{N_x}\sum_{j=1}^{N_y}\exp\left[-j\frac{2\pi}{\lambda}\triangle w_{\theta_0,\varphi_0}(\theta,\varphi)\right] \tag{12}$$

where

$$\triangle w_{\theta_0,\varphi_0}(\theta,\varphi) = \|\mathbf{d}_{ij}\|_x(\sin\theta\cos\varphi - \sin\theta_0\cos\varphi_0) + \|\mathbf{d}_{ij}\|_y(\sin\theta\sin\varphi - \sin\theta_0\sin\varphi_0)$$

3 Beam Direction Under Changed Satellite Attitude

For a given beam direction of (θ_0,φ_0), the omnidirectional antenna gain can be obtained by

$$G_{\theta_0,\varphi_0}(\theta,\varphi) = 20\log_{10}\|F_{\theta_0,\varphi_0}(\theta,\varphi)\| \tag{13}$$

where the maximum beam gain $G_t = G_{\theta_0,\varphi_0}(\theta_0,\varphi_0)$ is at the direction of (θ_0,φ_0). When a slight jitter occurs, the maximum beam gain shifts to another direction, e.g., (θ_1,φ_1). Therefore, the real beam gain at the target direction $G'_t = G_{\theta_1,\varphi_1}(\theta_0,\varphi_0)$ becomes

$$G'_t = 20\log_{10}\|\frac{1}{N_x \times N_y}\sum_{i=1}^{N_x}\sum_{j=1}^{N_y}\exp\left[-j\frac{2\pi}{\lambda}\triangle w_{\theta_1,\varphi_1}(\theta_0,\varphi_0)\right]\| \tag{14}$$

The beam gain loss at the target direction $\triangle G_t = G_t - G'_t$ is

$$\triangle G_t = 20\log_{10}\frac{\|\sum_{i=1}^{N_x}\sum_{j=1}^{N_y}\exp\left[-j\frac{2\pi}{\lambda}\triangle w_{\theta_0,\varphi_0}(\theta_0,\varphi_0)\right]\|}{\|\sum_{i=1}^{N_x}\sum_{j=1}^{N_y}\exp\left[-j\frac{2\pi}{\lambda}\triangle w_{\theta_1,\varphi_1}(\theta_0,\varphi_0)\right]\|} \tag{15}$$

Figure 3 shows the beam gain of a triangular grid phased array antenna. Assume that the jitter of satellite only change the value of θ, it can be observed that when the target θ changes, the beam gain loss for different φ is different. For example, in Fig. 3(a), the target UE is at the direction of $(5°, 90°)$, when θ changes to $10°$, the beam gain loss is nearly 3dB; in constant, as shown in Fig. 3(b), the target UE is at the direction of $(5°, 180°)$, when θ varies the same level, the beam gain loss is only 0.1dB. The aforementioned interesting phenomenon reveals that, there is always a best φ to make the beam most tolerant

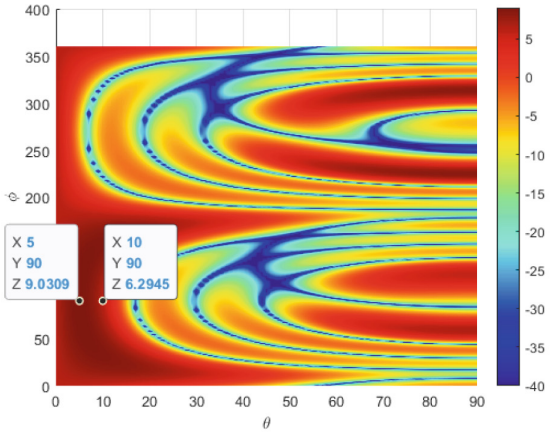

(a) The target beam direction is $(\theta, \varphi) = (5°, 90°)$

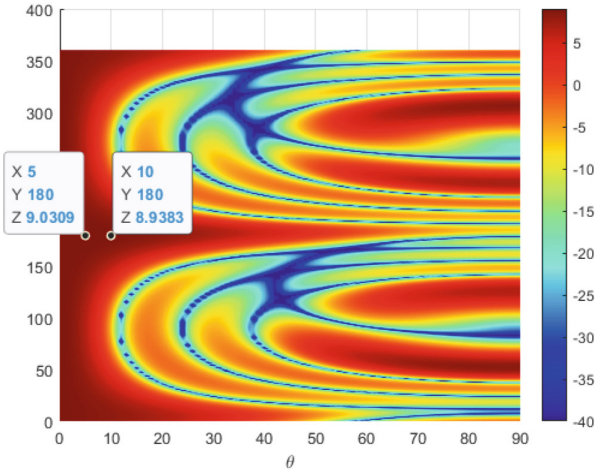

(b) The target beam direction is $(\theta, \varphi) = (5°, 180°)$

Fig. 3. Beam gain of a triangular grid array antenna with different direction.

for the variation of θ. Besides, satellite may change its attitude to enable the solar panel absorb more light energy. That leads to the antenna coordinate system not same as the orbit coordinate system. To describe the real-time attitude of the satellite, a local coordinate system should be established, and the two angles θ and φ should be calculated based on the local coordinate system. Moreover, three angles named the rolling angle α_x, the pitching angle α_y and the course angle α_z are used to describe the Euler angles between the local coordinate system and the orbit coordinate system. Normally, α_y and α_x are very small and the impact is negligible. In the following, we only consider α_z, and have

$$\varphi = \varphi_0 - \alpha_z \tag{16}$$

where φ_0 is the original azimuth and φ is the real azimuth after rotation. For satellite, the jitter is a random variable so that it is hard to know the exactly variation of θ, based on (16), one can obtain the best φ by adjusting the attitude of the satellite, so that the tolerant for the variation of θ can be guaranteed. The target is to find the optimal φ which can make the beam gain difference as little as possible when θ varies. So the cost function can be written as

$$\min_{\varphi} \{\triangle G_{\theta_1,\varphi}\} \tag{17}$$

where $\triangle G_{\theta_1,\varphi} = G_{\theta_1,\varphi}(\theta_1, \varphi) - G_{\theta_1,\varphi}(\theta_0, \varphi)$, where $\theta_1 = \theta_0 + \triangle\theta$, and $\triangle\theta$ is the elevation angle pointing error caused by the satellite jitter.

Consequently, to obtain the best φ which satisfy the cost function, a traversal method can be used. Set N as the number of iterations, the direction (θ_0, φ_0) of the targeted UE are used as the initial parameters of the searching process. The step of θ for each iteration is $\frac{360}{N}$. By comparing the beam gain loss $\triangle G_{\theta_1,\varphi_i}$ with the previous one, one can find the minimum $\triangle G_{\theta_1,\varphi_i}$ of the whole N times iterations. The proposed algorithm is summarized as the following Algorithm 4. Note that, to improve the search speed, some more efficient methods can be adopted, e.g., the binary search algorithm.

4 Simulations and Analysis

To evaluate the performance of the proposed algorithm, we take 4×2 triangular lattice array into consideration. As Fig. 4 illustrated, the distance on the horizontal direction is dx =20 mm and the distance on the vertical direction is dy =8.7 mm. The array antenna is equipped on a LEO satellite with orbit height of 500 km, and the six Keplerian elements of the orbit used for simulation are summarized in Table 1. With the parameters of the orbit, the orbital period is about 5690 s.

Algorithm 1. Optimal azimuth computation

Input: θ_0, φ_0, $\triangle\theta$, N.
Output: φ

initial $\varphi = \varphi_0$, $\theta_1 = \theta_0 + \triangle\theta$, $\triangle G_{\theta_1,\varphi_0} = G_{\theta_1,\varphi_0}(\theta_1, \varphi_0) - G_{\theta_1,\varphi_0}(\theta_0, \varphi_0)$,
for $i = 1$ to $N - 1$ **do**
  Compute $\varphi_i = (\varphi_0 + i \cdot \frac{360}{N})$;
  Compute G_{θ_1,φ_i} with beam direction of (θ_1, φ_i);
  Compute beam gain difference $\triangle G_{\theta_1,\varphi_i} = G_{\theta_1,\varphi_i}(\theta_1, \varphi_i) - G_{\theta_1,\varphi_i}(\theta_0, \varphi_i)$.
  if $\triangle G_{\theta_1,\varphi_i} < \triangle G_{\theta_1,\varphi_0}$ **then**
    $\triangle G_{\theta_1,\varphi_0} = \triangle G_{\theta_1,\varphi_i}$
    $\varphi = \varphi_i$
  end if
end for

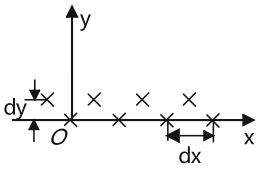

Fig. 4. Layout of 4×2 triangular grid array antenna.

Table 1. Parameters of the LEO orbit.

Eccentricity (e)	0
Semimajor axis (a)	6875800 m
Inclination (i)	2°
Longitude of the ascending node (Ω)	105.98°
Argument of periapsis (ω)	72°
mean anomaly (M)	0

For a target UE, the carrier to noise ratio (CNR) defined in [11] is adopted in order to evaluate the SNR at UE:

$$\text{SNR} = P_t + G(\theta, \varphi) + G/T - k - PL_{fs} - PL_{polar} - PL_{other} - 10\log_{10}(B) \quad (18)$$

where P_t, $G(\theta, \phi)$, G/T, k, B are the satellite transmit power, beam gain, antenna-gain-to noise-temperature, the Boltzmann constant, and the bandwidth, respectively. And the values used for simulation are shown in Table 2. Besides, PL_{fs}, PL_{polar} and PL_{other} are the path losses defined in [14].

Table 2. Simulation Parameters.

Satellite transmit power P_t	11 dBW
Antenna-gain-to noise-temperature G/T	19 dB/K
Boltzmann constant k	–228.6 dBW/K/Hz
Bandwidth B	200 MHz

In the simulation, we assume $\triangle\theta = \pm 5°$ and the number of iterations is $N = 360$. To evaluate the proposed algorithm, we use the SNR decrease as a metric to evaluate the performance loss caused by the jitter.

4.1 Nadir Point UE

In this subsection, we focus on the nadir point UE which is the intersection of the Earth center and the satellite's connection on the earth surface. Take the

nadir point of observation time $t = 2846\,s$ during the movement of satellite as the target UE position. At this time, the value of θ equals to zero. To ensure the minimum demodulation threshold, the dwelling time of satellite is defined as the time duration when $\theta < 53°$, i.e., from $t = 2744\,s$ to $t = 2946\,s$, as shown in Fig. 5. The value of θ would decrease as the satellite approaches to the UE and vice versa. In the dewelling time, the change of φ is very interesting: It can be seen that under the simulation assumption, φ keeps 360° when the satellite moves towards the UE, i.e., from 2744 s to 2845 s and φ keeps 180° when the satellite moves away from the UE, i.e., from 2846 s to 2946 s.

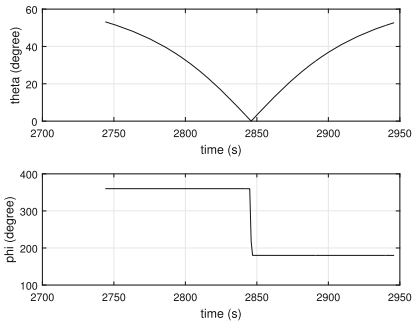

Fig. 5. Elevation and azimuth of the nadir point UE.

By employing the proposed algorithm, the value of original φ and the adjusted φ was shown in Fig. 6. Also, the corresponding total gain decrease with ±5° shift of elevation angle is presented. In Fig. 6, it presents that during the serving time, the beam gain performance decreases at least 2dB when θ changes ±5°. And the performance loss is as high as almost 6dB when satellite moves upon the target UE. That means with a fixed θ, the beam gain performance is always sensitive to the variation of θ no matter φ is 180° or 360°. Fortunately, this detrimental effect can be mitigated by our proposed algorithm. As can be seen, by updating the value of φ, even if the θ changes ±5° due to the jitter of satellite, the SNR loss reduces to no more than 0.18dB, which indicates that the proposed algorithm is robust for the θ error. Although the adjusted φ hops frequently between 90° and 270° during the dwelling time, it does not increase the complexity of satellite. This is because, the difference of the SNR loss between the two values is negligible due to the symmetrical character of antenna pattern. Thus, the optimal φ can be either of them without any angle switching, and besides, the computation can be done offline.

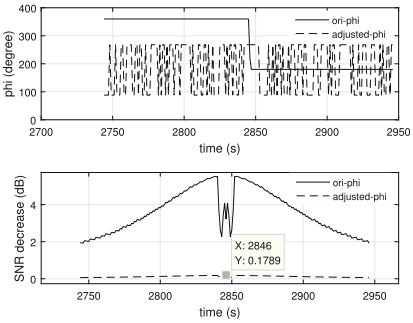

Fig. 6. Performance of the adjusted azimuth for the nadir point UE.

4.2 Non-nadir Point UE

In this subsection, we focus on the non-nadir point UE which is 500 km far away from the nadir point of observation time $t = 2846\,s$ as the UE position. As shown in Fig. 7, the azimuth angle φ varies from about 45° to 135°. The performance of the proposed algorithm is illustrated in Fig. 8. It can be seen that the azimuth angle φ is almost equals to the optimal φ when the satellite moves upon the target UE, so the SNR decrease of the real φ and the adjusted φ is almost the same. Simliar to the case of nadir point UE, the proposed algorithm can always obtain lower SNR decrease during the satellite dwelling time.

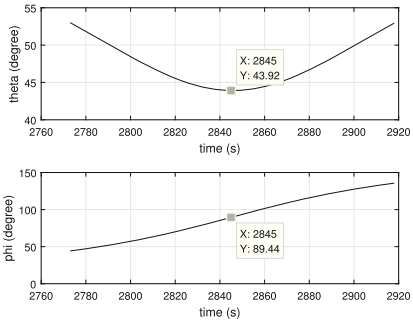

Fig. 7. Elevation and azimuth of the non-nadir point UE.

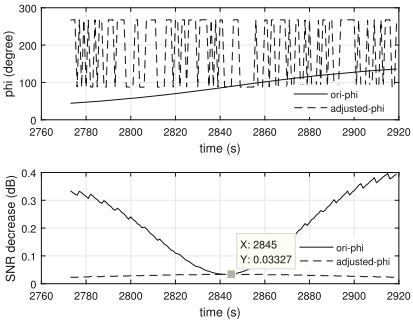

Fig. 8. Performance of the adjusted azimuth for the non-nadir point UE.

5 Conclusion

For triangular grid array, the antenna jitter may cause the difference of the real elevation angle and expected elevation angle, which leads to SNR loss of the target UE. To solve the problem, an adaptive azimuth adjustment algorithm is proposed. By carefully adjust the azimuth angle to the optimal direction, the SNR loss caused by the jitter is minimized and becomes negligible. Then the obtained optimal azimuth angle can be realized by changing the attitude of the satellite. Simulation results show the effectiveness of the proposed algorithm.

References

1. Kodheli, O., Lagunas, E., Maturo, N., et al.: Satellite communications in the new space era: a survey and future challenges. IEEE Commun. Surv. Tutorials **23**, 70–109 (2020)
2. 3GPP TR 38.811 V15.0.0. Study on new radio (NR) to support non-terrestrial networks
3. Liu, X., Lam, K.-Y., Li, F., Zhao, J., Wang, L., Durrani, T.S.: Spectrum sharing for 6G integrated satellite-terrestrial communication networks based on NOMA and CR. IEEE Netw. **35**(4), 28–34 (2021)
4. Shankar, B., Lagunas, M.E., Chatzinotas, S., Ottersten, B.: Precoding for satellite communications: why, how and what next? IEEE Commun. Lett. **25**, 2453–2457 (2021)
5. You, L., Li, K.-X., Wang, J., Gao, X., Xia, X.-G., Ottersten, B.: Massive MIMO transmission for LEO satellite communications. IEEE J. Selected Areas Commun. **38**(8), 1851–1865 (2020)
6. Moon, S., Yun, S., Yom, I., Lee, H.L.: Phased array shaped-beam satellite antenna with boosted-beam control. IEEE Trans. Antennas Propagation **67**(12), 7633–7636 (2019)
7. Kuhlmann, K., Jacob, A.F.: Antenna arrays on rectangular and triangular grids for polarization multiplexing - a comparative study. In: German Microwave Conference 2009, pp. 1–4 (2009)

8. Yun, Y., Jianshu, C., Jianchun, M.: Directional pattern modeling and simulation of triangular grid circular planar array antennas. In: 2010 2nd International Conference on Signal Processing Systems, pp. 666–669 (2010)
9. Rana, B., Lee, I.-G., Hong, I.-P.: Digitally reconfigurable transmitarray with beam-steering and polarization switching capabilities. IEEE Access **9**, 144140–144148 (2021)
10. Rahmat-Samii, Y., Densmore, A.C.: Technology trends and challenges of antennas for satellite communication systems. IEEE Trans. Antennas Propagation **63**(4), 1191–1204 (2015)
11. Toyoshima, M., Jono, T., Nakagawa, K., Yamamoto, A.: Optimum divergence angle of a Gaussian beam wave in the presence of random jitter in free-space laser communication systems. JOSAA **19**(3), 567–571 (2002)
12. Phelps, E., Primmerman, C.A.: Blind compensation of angle jitter for satellite-based ground-imaging lidar. IEEE Trans. Geosci. Remote Sens. **58**(2), 1436–1449 (2020)
13. Kim, I.I., Stieger, R., Koontz, J.A., Moursund, C., Barclay, M., et al.: Wireless optical transmission of fast ethernet, FDDI, ATM, and ESCON protocol data using the TerraLink laser communication system. Optical Eng. **37**, 3143–3155 (1998)
14. 3GPP TR 38.821 V16.0.0. Solutions for NR to support non-terrestrial networks (NTN)